

DENSITY FUNCTIONAL THEORY CALCULATIONS FOR FORMATION ENERGIES AND STRUCTURAL CHARACTERISTICS OF La OR Gd DOPED Bi_2WO_6 SYSTEMS

Tran Phan Thuy Linh¹, Pham Van Hai¹, Nguyen Dang Phu¹,
Duong Quoc Van¹, Nguyen Thi Thao¹ and Tran Thien Lan²

¹*Faculty of Physics, Hanoi National University of Education*

²*Vietnam-Japan University*

Abstract. By using first-principles calculations based on density functional theory, we investigate the doping effect of rare-earth elements (La and Gd) in Bismuth tungstate Bi_2WO_6 on structural characteristics. Firstly, the formation energies for doping configurations are calculated in order to carry out the most stable one. The obtained results prove that doping to sixteen Bi sites needs the similar formation energies due to the geometrical symmetry of the origin material. Secondly, the optimized structures of La- and Gd-doped systems are achieved by relaxation calculations. Finally, by comparison the lattice parameter between two doped systems, we find the insignificant changes in lattice constants, and hence, cell volumes. This can be attributed to the similarity in ionic radii of dopants (La or Gd) and host (Bi) ion.

Keywords: First-principles calculation, Bismuth tungstate, photocatalyst, dopant, formation energy, lattice parameter.

1. Introduction

Nowadays, the start of the industrial revolution with the exploitation and natural resources utilization excessively triggers the solemn problem in living environment. Photocatalytic semiconductor materials have been widely studied because of their remarkable properties for pollution remediation and hydrogen production from water splitting using solar energy [1-6]. Although photocatalysis efficiency has been broadly studied both experimentally and theoretically for decades, finding efficient photocatalyst is still the focus of many researchers. Presently, TiO_2 -based photocatalysts is mostly studied and efficient photocatalyst due to their high reactivity, good chemical stability, environmental friendly, and low cost [6-10]. However, the main limitation of

Received June 18, 2019. Revised June 22, 2019. Accepted June 29, 2019.

Contact Tran Phan Thuy Linh, email address: linhtpt@hnue.edu.vn

TiO₂ photocatalyst is intrinsic band gap (rutile 3.05eV, anatase 3.26eV), TiO₂ is able to be active only the ultraviolet part of the solar spectrum which accounts approximates only 3% to 4% of ultraviolet contribution [11]. Therefore, it is essential to develop novel visible-light-induced photocatalyst with high efficiency under normal solar light condition. Bi₂WO₆, a typical Aurivillius oxide with layered structure, has excellent intrinsic physical and chemical properties such as catalytic behavior, ferroelectric, pyroelectricity, piezoelectricity, oxide anion conducting and a nonlinear dielectric susceptibility [12-15]. Recently, Bi₂WO₆-based photo-catalysts have been widely studied for their promising photocatalytic performance under visible-light-irradiation [16-23]. Many experimental and theoretical publications have been performed to develop the photocatalytic efficiency of Bi₂WO₆ in the visible light region via doping in cationic sites (mostly Bi) since introducing doping states into the band gap and/or narrowing the latter. Furthermore, the doping into a semiconductor can create a new optical absorption edge which is very important in the photocatalysis process.

Therefore, in this paper, we focus on the formation of rare-earth element (M=La or Gd) doped Bi₂WO₆ systems. In order to find the favorite doping sites, the formation energies are calculated for 16 Bi possible doping configurations. The effect of dopants on crystal structure is elucidated. Besides, throughout this work, we use Visualization for Electronic and Structure Analysis (VESTA) to view the structure of our system.

2. Content

2.1. Computational method

Our predictions are obtained from the state of the art first-principles pseudopotential calculations based on Density Functional Theory (DFT) [24, 25] that is implemented in software package CASTEP [26]. Interactions of valence electrons with ion cores are modeled using projector augmented wave (PAW) [27] potentials. The plane-wave basis set is employed for the valence electron wave function with cut-off energy of 580 eV. Reference configurations of valence electrons were $6s^2 6p^3$ for Bi, $5d^4 6s^2$ for W, $2s^2 2p^4$ for O, $5d^1 6s^2$ for La and $4f^7 5d^1 6s^2$ for Gd. For the exchange-correlation energy, the generalized gradient approximation (GGA) was employed within the Perdew-Burke-Ernzerhof (PBE) [28] functional. The Brillouin zone was sampled using $2 \times 4 \times 7$ Monkhorst-Pack k-point grids [29] which showed total energy convergence within 1 meV per atom. The conjugate gradient minimization method was used to optimize all the atomic positions. Structural relaxation was terminated when the maximum Hellman-Feynman forces acting on each atom in the unit cell dropped to 0.001 eV/Å. The supercell $2 \times 1 \times 1$ was constructed by repetition of the unit cell of Bi₂WO₆. This supercell was composed of 72 atoms: 16 Bi atoms, 8 W atoms and 48 O atoms. Point defects were modeled by substituting one Bi site with a rare-earth atom so as to give a composition of Bi_{1.875}M_{0.125}WO₆ (M = La or Gd). The doping site was chosen so as to assemble the most stable configuration that possesses the smallest total energy, i.e. the lowest formation energy, in the relaxed structures among the all possible dopant configurations.

2.2. Results and discussions

2.2.1. Formation energy

The optimized supercell $2 \times 1 \times 1$ of Bi_2WO_6 consists 16 Bi atoms (Figure 1a) [30]. In order to find out the suitable doping site, the formation energies ΔH_f of sixteen M-doped Bi_2WO_6 configurations where M is substituted alternatively to sixteen possible sites of Bi cation were calculated. The smaller formation energy is, the more favorite doping site is. ΔH_f is defined as the energy needed to replace a Bismuth atom by an Lanthanum or Gadolinium atom, and is calculated as follows [31]:

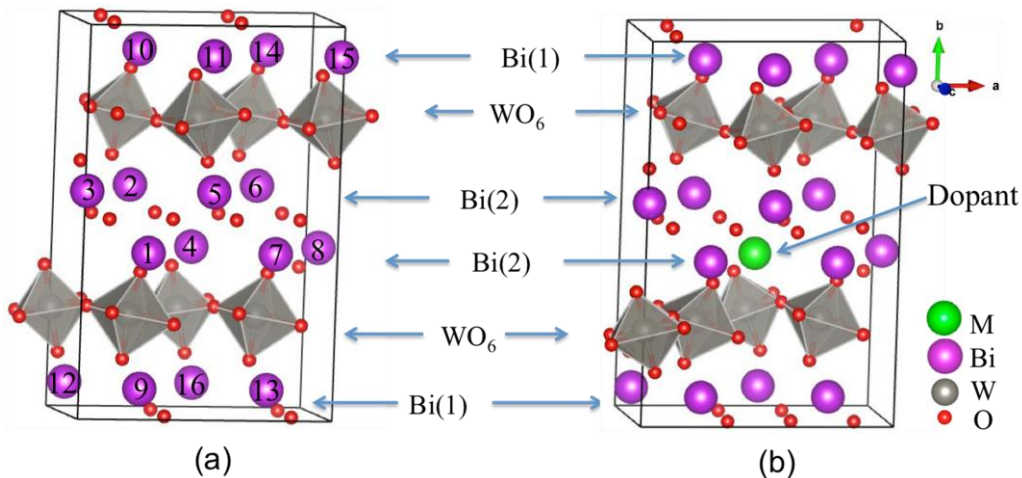


Figure 1. Crystal structure of supercell undoped and M-doped Bi_2WO_6 . Gray octahedra indicate WO_6 substructures. A black solid box presents a boundary of the super-cell

$$\Delta H_f = E_{tot} - \sum_i \mu_i x_i \quad (1)$$

where, E_{tot} is the DFT total energy of the doped compound, μ_i is the chemical potential of element i , and x_i is the quantity of element i in the compound.

We firstly perform DFT calculations so that the total energies of all possible doped configurations are carried out. Then the formation energies are obtained from equation (1) and are listed in Table 1. It can be seen from Table 1 that the discrepancy in average values of formation energies of La- and Gd-doped systems is only 0.1% (about -1.82171 eV and -1.81925 eV for La- and Gd-doped systems, respectively). Moreover, in each doped system, the energy differences between the many possible configurations are not large (about 0.0001 eV) for both La-doped and Gd-doped Bi_2WO_6 . This can be attributed to the geometrical symmetry of the pure system Bi_2WO_6 that sixteen Bi cations are all located in equivalent positions. Therefore, our next calculation will focus on only one doped configuration where the Bi4 site is substituted by a La/Gd atom (Figure 1b).

Table 1. Formation energy (eV) of sixteen possible configurations of M-doped Bi₂WO₆ systems

Doping site	La-doped	Gd-doped
Bi1	-1.82179	-1.81928
Bi2	-1.82179	-1.81928
Bi3	-1.82179	-1.81929
Bi4	-1.82182	-1.81929
Bi5	-1.82179	-1.81928
Bi6	-1.82179	-1.81928
Bi7	-1.82179	-1.81929
Bi8	-1.82179	-1.81929
Bi9	-1.82161	-1.81922
Bi10	-1.82176	-1.81922
Bi11	-1.82161	-1.81922
Bi12	-1.82161	-1.81922
Bi13	-1.82161	-1.81922
Bi14	-1.82161	-1.81922
Bi15	-1.82161	-1.81922
Bi16	-1.82161	-1.81922

3.2. Structural characteristics

The optimized structures of undoped and doped systems, respectively, Bi₂WO₆ and Bi_{1.875}M_{0.125}WO₆ (M = La or Gd), are evaluated by relaxation calculations. For all systems, we optimized both the cell shape and cell volume. The lattice parameters of optimized structures with La or Gd dopants are listed in Table 2. The M-doped Bi₂WO₆ systems remained orthorhombic system, space group Pca2₁, with the WO₆ octahedral layers and the Bi–O–Bi layers, the same as undoped Bi₂WO₆. The lattice constants, in general, decreased for the *b* axis, but increased for *a* and *c* axes. The decrease of *b* axis of the La-doped system is insignificant, and that of Gd-doped system is about 0.4%. The increases for the *a* and *c* axes of the La-doped system are about 0.2% and 0.16%, respectively; while those values of Gd-doped system is insignificantly. Thus, the cell volume is increased by 0.2% for La-doped system, but decreased by 0.3% for Gd-doped system. Those changes resulted from the difference in ionic radii of dopant (1.032 Å and 0.938 Å for La³⁺ and Gd³⁺ respectively) host (1.03 for Bi³⁺) [32]. Due to the slight difference in cell shape and cell volume between undoped and doped systems, we expect that there is no significant elastic strain in the crystal structure in doped systems and structural relaxation only affects the local surrounding of the defects in the actual materials. The comparison of the coordinate of each atom and that of W–O bond lengths in each octahedron are accomplished and verify our prior expectation.

Table 2. Structure parameters of undoped and La- or Gd-doped Bi₂WO₆ systems

	Lattice constant/Å			Angle/deg.			Cell vol./ Å ³
	<i>a</i>	<i>b</i>	<i>c</i>	α	β	γ	
Undoped	11.1227	16.8683	5.6049	90.0000	90.0000	90.0000	1051.6132
La-doped	11.1517	16.8357	5.6138	89.7751	90.0986	89.9155	1053.9734
Gd-doped	11.1229	16.8026	5.6076	90.2281	89.9393	90.0454	1048.0275

3. Conclusions

First-principles calculations of M-doped Bi₂WO₆ (M = La or Gd) show that the crystal structure of orthorhombic undoped Bi₂WO₆ *Pca*2₁ space group is maintained by the doping. Due to the similarity in ionic radius between La (Gd) and host Bi, the unit cell volume of La (Gd)-doped system changes only 0.2% (0.3%). Thus there is no important elastic strain in doped systems by structural relaxation. The effect of these dopants on electronic properties of Bi₂WO₆ will be considered in our next work.

Acknowledgements. The authors would like to thank the Ministry of Education and Training of Vietnam (MOET), Grant B2018-SPH-04-CTrVL for financial support.

REFERENCES

- [1] X. Lang, X. Chen, J. Zhao, 2014. Chem. Soc. Rev., 43, 473.
- [2] M.Y. Guo, A.M.C. Ng, F. Liu, A.B. Djurišić, W.K. Chan, 2011. Appl. Catal. B: Environ., 107, 150.
- [3] J. Yu, Y. Yu, P. Zhou, W. Xiao, B. Cheng, 2014. Appl. Catal. B Environ., 156.
- [4] T. A. Kandel, K. Takanabe, 2016. Appl. Catal. B Environ., 184, 264.
- [5] H. Ait ahsaine, A. El jaouhari, A. Slassi, M. Ezahri, A. Benlhachemi, B. Bakiz, F., 2016. Guinneton and J. R. Gavarri, RSC Adv., DOI: 10.1039/C6RA22669H.
- [6] M.J. Esswein, D.G. 2007. Nocera, Chem. Rev., 107.
- [7] X. Chen, S.S. Mao, 2007. Chem. Rev., 107.
- [8] J.N. Schrauben, R. Hayoun, C.N. Valdez, M. Braten, L. Fridley, J.M. Mayer, 2012. Science 336.
- [9] Q.J. Liu, Z. Ran, F.S. Liu, Z.T. Liu, J. 2015. Alloys Compd. 631.
- [10] Nguyen Dang Phu, Luc Huy Hoang, Xiang-Bai Chen, Meng-Hong Kong, Hua-Chiang Wen, Wu Ching Chou, 2015. Journal of Alloys and Compounds, 647, 123.
- [11] Y. Houman, L. Zhi, C. Yao, T.N. Huong, R.B. Venkat, J. Babu, S.Q. Ma, S. Rudy, T.T. Arash, 2015. ACS Catal., 5, 327.
- [12] Ran Chen, Chaohao Hu, Shuai Wei, Jinhong Xia, Jian Cui and Huaiying Zhou, 2013. Mater. Sci. Forum, Vols 743-744, p. 560.
- [13] A. Taoufyq, B. Bakiz, A. Benlhachemi, L. Patout, D. V. Chokouadeua, F. Guinneton, G. Nolibe, A. Lyoussi, J-R. Gavarri, 2015. World Academy of Science,

Engineering and Technology International Journal of Chemical and Molecular Engineering, Vol. 9, No. 2.

- [14] Y. Shi, S. Feng, C. Cao, 2000. *Mater. Lett.*, 44.
- [15] P. Ju, P. Wang, B. Li, H. Fan, S. Ai, D. Zhang, Y. Wang, 2014. *Chem. Eng. J.*, 236.
- [16] D.X.Wu, H.T.Zhu, C.Y.Zhang, L.Chen, 2010. *Chem.Comm.*, 46.
- [17] G. Zhao, S. Liu, Q. Lu, F. Xu, H. Sun, 2013. *J. Alloys Compd.*, 578.
- [18] M.Shang, W.Wang, J.Ren, S.Sun, L.Wang, L.Zhang, 2009. *J.Mater.Chem.*,19.
- [19] F. Amano, K. Nogami, B. Ohtani, 2009. *J. Phys. Chem.*, C 113.
- [20] D. Ma, S. Huang, W. Chen, S. Hu, F. Shi, K. Fan, 2009. *J. Phys. Chem.*, C 113.
- [21] Y. Huang, Z. Ai, W. Ho, M. Chen, S. Lee, 2010. *J. Phys. Chem.*, C 114.
- [22] S.P. Hua, C.Y. Xu, L. Zhen, 2013. *Mater. Lett.*, 95.
- [23] X. Wang, P. Tian, Y. Lin, L. Li, 2015. *J. Alloys Compd.*, 620.
- [24] W. Kohn and L. J. Sham, 1965. *Phys. Rev.*, Vol. 140, p. A1133.
- [25] G. Kresse and J. Hafner, 1993. *Phys. Rev. B*, Vol. 47, p. 558.
- [26] J. Clark Stewart, *et al.*, 2005. *First principles methods using CASTEP*. *Z. für Kristallogr. - Cryst. Mater.*, 220 (5/6) 567-570.
- [27] Blochl, P. E. 1994. *Projector Augmented-Wave Method*. *Phys. Rev. B*, 50, 17953.
- [28] Perdew, J. P.; Burke, K. 1996. *Ernzerhof, M. Generalized Gradient Approximation Made Simple*. *Phys. Rev. Lett.*, 77, 3865.
- [29] Monkhorst H J and Pack J D, 1976. *Phys. Rev.*, B 13, 5188.
- [30] T. P. T. Linh, P. V. Hai, N. D. Phu, D. Q. Van, N. T. Thao and T. T. Lan, 2018. *HNUE Journal of Science, Natural Sciences*, 63 (11), p. 71.
- [31] Scott Kirklin, James E Saal, Bryce Meredig, Alex Thompson, Jeff W Doak, Muratahan Aykol, Stephan Rühl and Chris Wolverton, 2015. *Npj Computational Materials*, 1, 15010; published online 11 December 2015.
- [32] Shannon R D, 1976. *Acta. Cryst.*, A **32**, 751.